Journal of the European Ceramic Society 22 (2002) 2587–2593

www.elsevier.com/locate/jeurceramsoc

Microstructure of hot-pressed Ti(C,N)-based cermets

Frederic Monteverde*, Valentina Medri, Alida Bellosi

National Research Council, Research Institute for Ceramics Technology, Via Granarolo, 64, 48018 Faenza, Italy

Received 20 October 2001; received in revised form 10 February 2002; accepted 28 February 2002

Abstract

Starting from commercial nanosize TiN and carbon black powders, this study set up a synthesis of fine and pure Ti(C,N) powders. The best experimental conditions were found using a mixture TiN + 10 wt.% of C processed at 1430 °C for 3 h under flowing Argon. The as-produced Ti(C,N) powder showed regularly shaped particles (100–300 nm), little agglomeration and a C/(C + N) atomic ratio ranging from 0.4 to 0.6. A mixture of Ti(C,N) + 15.3 wt% of WC and 9.1 wt% of Ni + Co was prepared and hot pressed at 1620 °C for 30 min (5 MPa of applied pressure). Microstructure and some properties of the sintered ceramic–metal composite (cermet) was investigated by SEM-EDX and XRD. The material exhibited a refined microstructure, but also the presence of textured flaws of several tenths of microns, attributed to not-optimized sintering conditions. The results were compared with those obtained from a cermet manufactured with the same nominal formulation but with commercial $TiC_{0.5}N_{0.5}$ raw powder.

Keywords: Hot pressing; Microstructure-Final; Powder-solid state reaction; Titanium carbonitride; X-ray method

1. Introduction

Titanium carbonitrides are widely applied as the hard phase in sintered ceramic–metal composites (cermets) and for protective coatings on conventional hardmetal substrates. An excellent and unique combination of physical properties like high melting point, hardness, thermal conductivity, wear resistance, good chemical and wear resistance make this family of structural and wear-resistant materials rather attractive in the field of cutting tools.[1–7] This type of modern Ti(C,N)-based hardmetals has been successfully employed in high speed finishing operations on high strength steel grades and ductile cast irons but reduced cross section of the chips.[1] In comparison to WC-Co conventional inserts, this class of materials has improved surface finishing, ensuring at the same time excellent chip and tolerance control and the dimensional accuracy of the workpieces.[6] Designed additions of carbides (i.e. WC, Mo_2C, NbC, TaC) into Ti(C,N)-based mixtures have become a standard step of the manufacturing route which enables adjustment of desirable physical and mechanical properties in order to match specific requirements during cutting operations.[1–5,8–13] Furthermore, the introduction of metallic binders (i.e. Ni, Co) fulfils the twofold need to improve fracture toughness and to activate densification mechanisms during sintering.[1,3,4,14]

The resulting microstructure of Ti(C,N)-based cermets depends on the type and amount of carbides and metallic dopants. Moreover the final characteristics of the hard phases and binder are greatly affected by the composition of the starting mixture and by the processing conditions. The mutual solubility during sintering of the phases involved plays a decisive role on the microstructure development.[1,3,4,9–14]

The role of the starting Ti(C,N) powders, grain size distribution and stoichiometry have to be strictly controlled. Several methods for the production of raw Ti(C,N) powders were reported, specifically from solid,[5,15–18] liquid,[5] and gaseous state.[1,5,19] The carbothermal reduction from TiO_2 is one of the cheapest routes for the synthesis of TiN, TiC or Ti(C,N) powders.[15–17] However scarce control of particle size distribution and the low purity level of the final products still represent undesirable drawbacks of this fabrication process.

This study focuses two aspects:

1. to set up a synthesis of ultrafine (particle size <0.2 μm) and highly pure Ti(C,N) powders (i.e

* Corresponding author. Tel.: +39-0546-699758; fax +39-0546-46381.

E-mail address: federico@irtec1.irtec.bo.cnr.it (F. Monteverde).

0955-2219/02/$ - see front matter
PII: S0955-2219(02)00120-6

no residual free carbon), with little agglomeration and an atomic ratio C/(C + N) approaching to 0.5, starting from commercial nanosize TiN and carbon black powders.
2. to produce and characterize dense Ti(C,N)-based cermets starting from the as-produced Ti(C,N) powders, mixed with WC-Co, Ni and Co.

Densification behaviour, microstructure and properties were analyzed and compared with those of a cermet fabricated from a commercial $TiC_{0.5}N_{0.5}$ powder with the same percentage of additives.

2. Description of the Ti(C,N) phase

TiN and TiC are two interstitial compounds of titanium which possess a B1-NaCl type crystal structure. These binary f.c.c. phases form complete quasi-binary Ti(C,N) solid solutions with the atoms of carbon and nitrogen at all the octahedral interstitial lattice sites.[1,5,20] Such a compound can be simply classified as a perfect solid solution TiC_YN_X ($X+Y=1$) between two vacancy-free boundary phases TiC and TiN. Actually the relative stability of nitrogen in the TiC_YN_X solid solution and the sensitive dependence of the energy of formation on the composition (i.e. C/C + N ratio) require the need of a model of solid solution that takes adequately into account the departure from an ideal behaviour.[21]

3. Experimental

3.1. Powder processing and densification

Some characteristics of the starting commercial powders are shown in Table 1. A mixture TiN + 10wt.% of carbon black was ultrasonicated in *n*-hexane, dried with a rotating evaporator, sieved and pelletized (1000 kg/cm^2). The solid-state synthesis of Ti(C,N) from the TiN/C mixture was conducted at 1430 °C for 3 h in flowing Argon (heating rate 10 °C/min, free cooling down) using a graphite crucible in a heated graphite chamber (carefully purged with Argon before heating). The as-obtained Ti(C,N) powder (named TiCN1) was homogeneized with the additives (wt.%), 15.3WC(Co) + 6.2 Ni + 2.1Co, in pure ethanol for 48 h using WC milling media, and then dried and sieved. The same composition was prepared from a commercial $TiC_{0.5}N_{0.5}$ powder.

Both the mixtures were consolidated by hot pressing, using the processing parameters summarized in Table 2, where the two dense cermets are labelled HP1 and HP2. The ram displacement was recorded on-line during hot pressing and densification curves were then calculated.

3.2. Powder characterization

Morphological and structural analyses were performed on the powders. For practical purposes, the Ti(C,N) phase was modelled as a perfect $TiC_{1-X}-TiN_X$ solid solution with a B1-NaCl type structure. On these basis, the atomic content of carbon (i.e. 1−X) or nitrogen (i.e. *X*) was estimated from the cubic Ti(C,N) cell parameter $a_{Ti(C,N)}$, extrapolated from XRD patterns with the Nelson–Riley function[22] and accordingly with the Vegard's rule: $a_{Ti(C,N)}=(1-X)a_{TiC}+Xa_{TiN}$ where $a_{TiC}=0.43274$ nm (ICDD card 32–1383), $a_{TiN}=0.42417$ nm (ICDD card 38–1420). Moreover, on the basis of the ideal TiC_{1-X}/TiN_X mixing model proposed by Pastor,[5] the domains of stability of the $TiC_{1-X}N_X$ phase at various temperatures were calculated. These diagrams define the range of the nitrogen partial pressure in order to optimize the experimental conditions for the synthesis. Multicomponent equilibrium calculations were simulated as well by means of the software package HSC 4.1.[23]

3.3. Characterization of the dense cermets

The density of the sintered samples was measured by the Archimedes method, whereas the final relative density was estimated in accordance with the rule of the powder mixtures. Morphology, composition and distribution of the present phases were investigated by XRD (with Ni-filtered $Cu_{K\alpha}$ radiation) and SEM-EDX equipments.

Vickers microhardness (HV) tests were conducted, using a load of 1 kg (10 s of loading time). Fracture toughness (K_{IC}) was evaluated by the direct crack-

Table 1
Main characteristics of the starting powders: specific surface area (s.s.a)

Powder	Company	s.s.a (m^2/g)	Chemical composition (wt.%)		
TiN	H.C. Starck	23.6	O: 0.7	Cl:0.5	C:0.08
Carbon black	Degussa	113	–	–	–
$TiC_{0.5}N_{0.5}$	H.C. Starck	3.3	O:0.9	C_{free}:0.1	–
WC-5Co	Nanodyne	0.9	Co:5.24	C_{free}: 0.04	<0.002
Ni,Co	Sherrit	–	–	–	–

All values come from datasheets of the producers.

Table 2
Processing parameters of the hot press runs: sintering temperature T_S, dwell time *t*, onset temperature T_{ON}, applied pressure 5 MPa

Label	Ti(C,N) powder			T_S (°C)	*t* (min)	T_{ON} (°C)
	Type	s.s.a (m^2/g)	*X*			
HP1	TiCN1	4.9[a]	0.4÷0.6	1620	30	1460
HP2	$TiC_{0.5}N_{0.5}$	3.3	0.5	1650	45	1450

[a] Internal measurement.

measurement method (98.1 N applied load, 10 s loading time) on the polished surfaces, using the model proposed by Evans et al.[24]

4. Results and discussion

4.1. Synthesis of the Ti(C,N) powder

Titanium carbonitride is obtained from the following reaction between the titanium nitride and carbon:

$$TiN + (1 - X)C \rightarrow TiC_{1-X}N_X + \left(\frac{1}{2} - X\right)N_2(g) \uparrow \qquad (1)$$

After several tests at different temperatures and dwell times, the best compromise among the processing conditions was found at 1430 °C for 3 h in flowing Argon, as previously described.[25] Morphology and particle size of the as-synthesized TiCN1 powder are compared with the commercial $TiC_{0.5}N_{0.5}$ powder in Fig. 1. The specific surface area (s.s.a) of the TiCN1 powder, measured with the Brunauer-Emmett–Teller method, resulted 4.9 m^2/g. After the standardized procedure of smoothing–background purging–$K_{\alpha 2}$ stripping of the unprocessed XRD pattern, the coexistence of, at least, two $TiC_{1-X}N_X$ phases with diffxerent stoichiometry, $0.4 < X < 0.6$ (Table 2), was assessed. Actually, a closer examination of the profiles of the elaborated pattern seemed to highlight the presence of weaker overlapped peaks, likely associated to $TiC_{1-X}N_X$ with proper X parameters. The calculation of the multiphase equilibrium of the reaction (1) (Fig. 2) and of the domain of stability at 1430 °C[5] do not exclude the formation of stable Ti(C,N) phases with different C(C + N) atomic ratio.

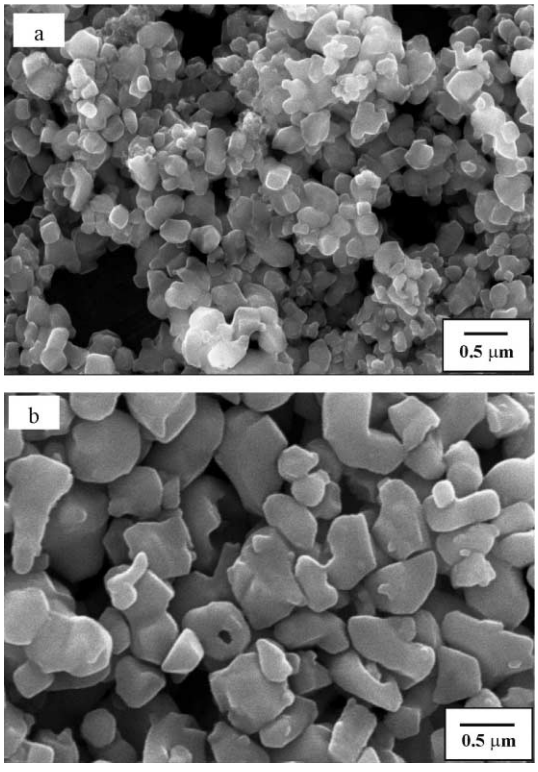

Fig. 1. (Secondary electron)-SEM micrographs of the raw Ti(C,N) powders used, TiCN1 (a) and $TiC_{0.5}N_{0.5}$ (b).

4.2. Densification behaviour during hot pressing

The densification plots vs temperature and time of material HP1 and HP2 are compared in Fig. 3. This class of cermet alloys is known to sinter in the presence of a liquid phase.[1,3,4,14] After particle rearrangement (negligible shrinkage), liquidus formation occurred at the onset temperature T_{ON} (Table 2), inducing a drastic shrinkage of the green body. Increasing the temperature, particularly above 1550 °C, the liquidus reached the maximum volume and had a reduced viscosity, so rapid densification took place and the compact achieved nearly full density (Table 3). The sudden raise of the densification rate at T_{ON} is a clear indicator of the occurrence of an eutectic liquid phase, based on the metallic dopants (i.e. Ni and Co). The densification behaviour of the two materials is slightly different, probably due to the enhanced reactivity of the finer TiCN1 powder (Fig. 1) and to different starting X values (Table 2). It is known in fact that, apart temperature and processing atmosphere, the metallurgical reactions involved during the liquid phase sintering are greatly influenced by the nitrogen activity in the dissolving Ti(C,N) particles which, in turn, is controlled by their stoichiometry.[1–5,8–14]

4.3. Microstructure of the two dense cermets

Both the materials HP1 and HP2 exhibit a core/rim structure embedded into a metal binder network (Fig. 4).

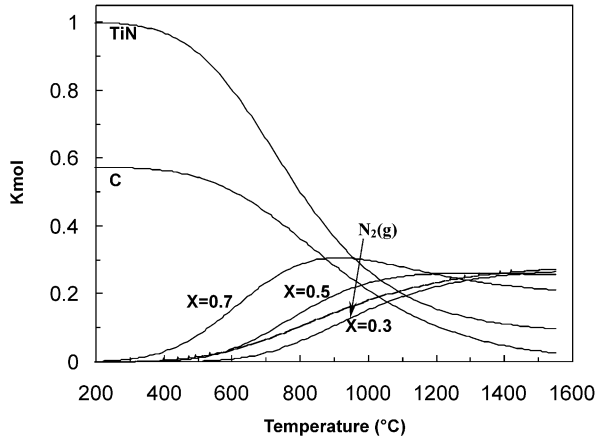

Fig. 2. Multicomponent equilibrium calculation (at 10^{-4} bar) of the reaction (1). The thermodynamic database was updated for the $TiC_{1-X}N_X$ solid solutions considered.

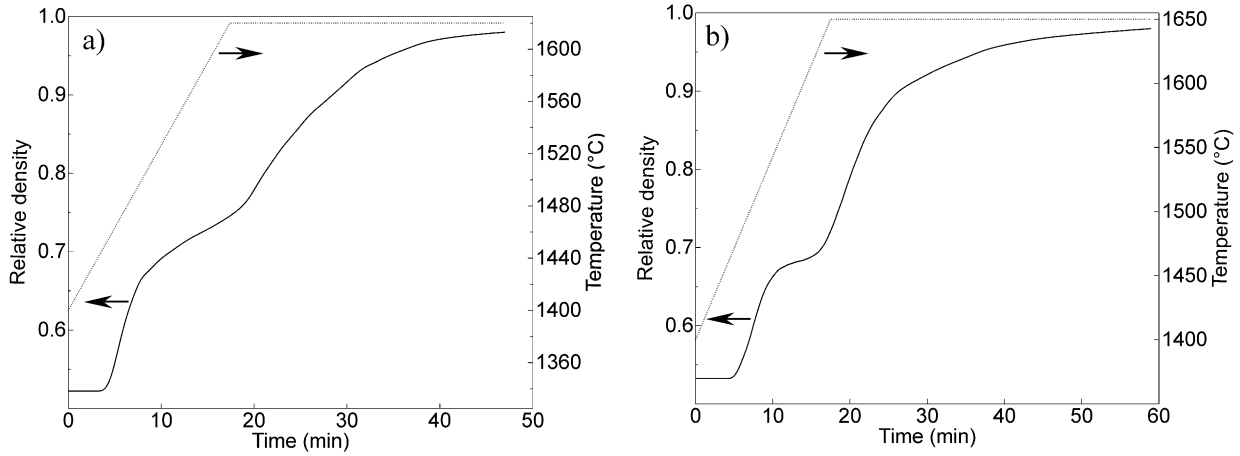

Fig. 3. Densification plots vs. temperature/time of material HP1(a, 1620 °C for 30 min) and HP2 (b, 1650 °C for 45 min).

Table 3
Some microstructural parameters of the sintered cermet alloys: theoretical density ρ_T, Archimedes density (ρ_A), final relative density ρ_{REL}, and (cubic) cell parameter

Material	ρ_T (g/cm^3)	ρ_A (g/cm^3)	ρ_{REL} (%)	(fcc) Crystalline phases[a]	Cell parameters (nm)		
					Rim	Core	Binder
HP1	6.0	5.87	97.8	Core, rim, binder	0.4280	0.4273	0.356
HP2	5.93	5.82	98.0	Core, rim, binder	0.4286	0.4281	0.354

[a] Core: Ti(C,N); rim: (Ti,W)(C,N); binder: Ni–Co–Ti–W.

An illustration of this typical microstructure is sketched in Fig. 5. The cores consist of partly undissolved raw Ti(C,N) particles, onto which (Ti,W)(C,N) rims have grown through a dissolution–reprecipitation mechanism during sintering.[26] The sintering conditions, particularly the processing atmosphere, influenced grain growth (i.e. size of the rim) and composition of the mentioned features (i.e the amount of C, N and solutes in the core, rim and binder).[1,3,4,8,11,14] A closer inspection of the microstructure also revealed an inner rim which often is located at the interface between the core and the outer rim (Figs. 4 and 5). Material HP2 reached full density (Table 3) and no remarkable porosity or defects were found.

In the case of material HP1, relatively large microstructural defects (Fig. 6) were revealed. The occurrence of such widespread and textured flaws was primarily caused by the reduction of the sintering temperature (30 °C less) and soaking time (15 min less) that ultimately hindered the densification mechanisms previously

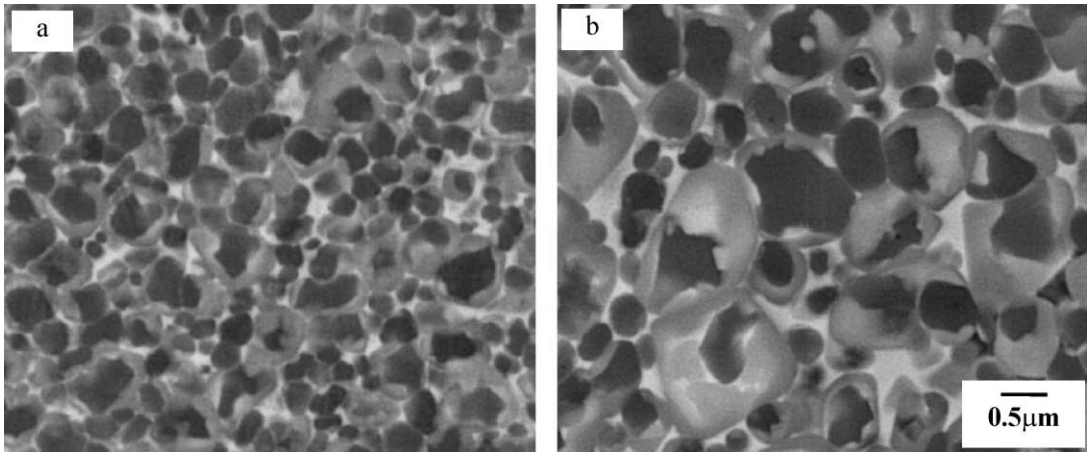

Fig. 4. (Back scattered electron)-SEM micrographs from polished section of material HP1 (a) and HP2 (b).

described. Moreover, the identification of areas (named grey network in Fig. 7) with stoichiometry close to that of the outer rim but still containing also nickel and cobalt may support the hypothesis that the liquid phase sintering process, in HP1, was prematurely stopped. In both the sintered cermets, the core contains only titanium, carbon, and nitrogen, while tungsten is present in the outer rim (Fig. 8). The atoms of W in fact entered into the Ti(C,N) lattice during heat treatment and replaced titanium at the metallic sublattice sites.[11,12,26]

For both the materials, the isomorphism of the (cubic) crystalline core and the outer rim was confirmed by nearly overlapped XRD patterns in the forward angular range. A careful XRD inspection scanned along the back-reflection angular range (Fig. 9) allowed to discriminate and then to measure small cell-parameter misfit between the core and outer rim (Table 3). Little lattice dilatation results from the entrance of tungsten into the Ti(C,N) lattice.[27] On the support of a vacancy-free $TiC_{1-X}N_X$ solid solution which obeys the Vegard's rule, the stoichiometric coefficient X was directly estimated and, in the case of material HP2, resulted in $X \approx 0.5$. For material HP1, the cell parameter (Table 3) of the cores is shorter: EDX analyses confirmed the result of N-richer Ti(C,N) starting powders (Fig. 10). On the other hand, the presence of heavy W atoms in the outer rim causes an appreciable departure from the ideal behavior.[28] Therefore, the model of a perfect solid solution cannot adequately provide reliable information on the amount of the atomic species contained in the (Ti,W)(C,N) solid solution rim.

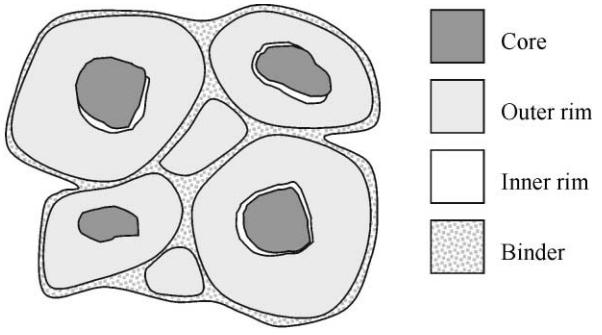

Fig. 5. Schematics of the core/rim structure.

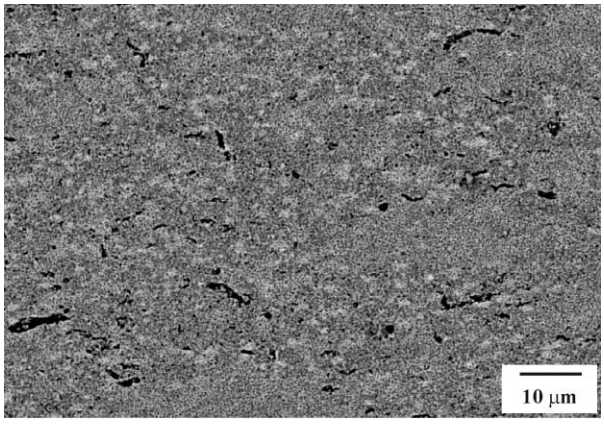

Fig. 6. (Back scattered electron)-SEM micrographs from polished section of material HP1: the dark textured features consist of residual flaws.

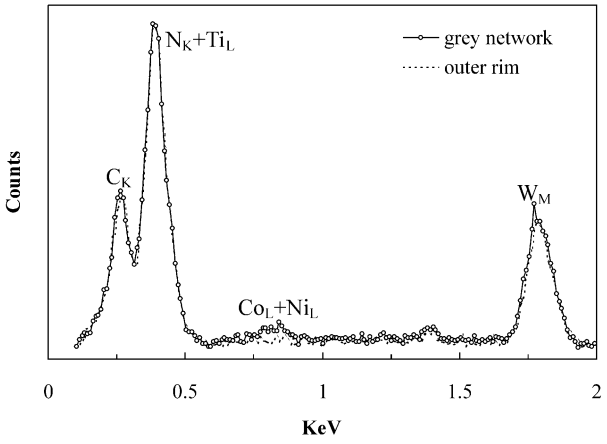

Fig. 7. Comparison of the EDX spectra (electron beam energy 8 KeV) from the "grey newtork" and an outer rim of material HP1.

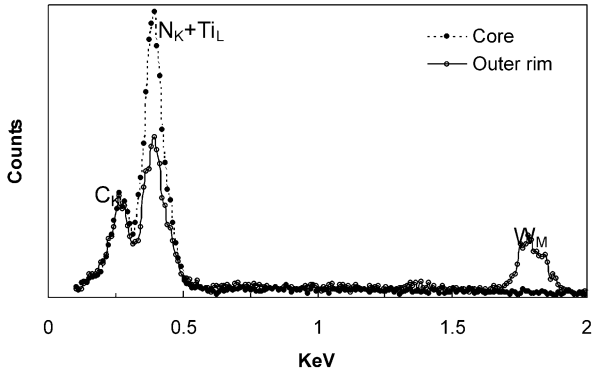

Fig. 8. Comparison of EDX spectra (electron beam energy: 8 KeV) from a core and an outer rim of the material HP1.

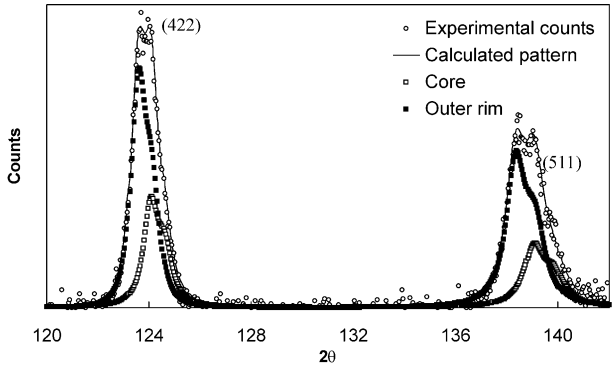

Fig. 9. Experimental and calculated XRD patterns of material HP1: single contributions from the core and the outer rim are shown.

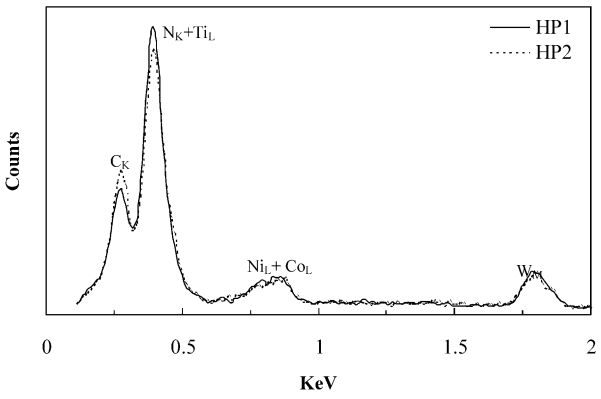

Fig. 10. EDX spectra (electron beam energy 8 KeV) of cermet HP1 and HP2, acquired from a representative area of the overall composition.

In material HP1, the lower sintering temperature (i.e. 1620 °C) and the N-rich starting stoichiometry slowed down the dissolution–repricipitation mechanisms,[29] decreasing grain growth in respect with material HP2 (Fig. 4).

The brighter appearance, in the BSE mode (Fig. 4), of the inner rim is due to the enrichment in tungsten. That inner rim in fact supposedly originates during the earliest stage of sintering, when WC interacts on contact with the cobalt binder, through a solid-state reaction (the liquidus is not yet formed), and a large quantity of tungsten is available.[14] Therefore, the inner rim represents the memory of the complete dissolution of the WC before a massive liquid-phase sintering.

The binder phase is well distributed as a thin layer around the hard ceramic grains. Its composition falls into the Ni–Co–Ti–W system and it has a cubic symmetry with a cell parameter (Table 3) in agreement with the literature data.[12]

4.4. Mechanical properties

The experimental values of the mechanical properties are reported in Table 4. The material HP1, although having a smaller grain size, was softer than HP2 because of the existence of relatively large flaws (Fig. 6) and a TiN-richer overall composition (Fig. 10). It is known in fact TiC-richer matrices guarantee harder components.[30] However the values of the fracture toughness, calculated using the model of Evans and Charles,[24] do not differ significantly.

Table 4
Microhardness (HV) and fracture toughness (K_{IC}) of the tested cermets

Material	HV (GPa)	K_{IC} (MPa$\sqrt{m}$)
HP1	14.9±0.5	5.5±0.3
HP2	16.8±0.3	5.8±0.2

5. Conclusions

The study set up a route to produce very fine Ti(C,N) powders. The solid state synthesis of Ti(C,N) was performed at 1430 °C for 3 h in flowing Argon, starting from a mixture of commercial nanosize TiN powders + 10 wt.% of carbon black. The produced powders exhibited rather regular shape, submicrometric size, little agglomeration and an atomic ratio C/C + N in the range 0.4–0.6.

This powder was then mixed with 15.3 wt.% of WC(Co) + 6.2 wt.% of Ni + 2.1 wt.% of Co and hot-pressed. Such a dense cermet was compared with another material obtained from commercial $TiC_{0.5}N_{0.5}$ powder, and using the same content of additives. For both the materials, the liquid phase sintering activated the dissolution–repricipitation mechanism and nearly full density was achieved.

These cermet alloys showed the typical core/rim structure embedded in a metal binder network. The cores consist of undissolved Ti(C,N) particles onto which (Ti,W)(C,N) rims precipitated from the liquid phase and grew up. The atomic ratio C/C + N of the starting powders and the processing conditions greatly influenced microstructure, distribution and composition of the present phases. The material obtained from the homemade Ti(C,N) powder exhibited a refined microstructure, but also the presence of textured flaws of several tenths of microns, attributed to not-optimized sintering conditions.

Acknowledgements

The work was sponsored by MURST and CNR under the National Project "Innovative Materials", Law 95/95–5%. The authors thank Dr. G. Celotti and Dr. F. Rinaldi for their helpful contribution on the XRD analyses.

References

1. Lengauer, W., Transistion metal carbides, nitrides, and carbonitrides. In *Handbook of Ceramic Hard Materials*, ed. R. Riedel. Wiley-VCH Verlag GmbH, Weinheim, 2000, pp. 203–252.
2. Clark, E. B. and Roebuck, B., Extending the application areas for titanium carbonitride cermets. *Refr. Met. & Hard Mat.*, 1992, **11**, 23–27.
3. Zhang, S., Material development of titanium carbonitride-based cermets for machining application. *Key Engineering Materials*, 1998, **138–140**, 521–543.
4. Ettmayer, P., Kolaska, H., Lengauer, W. and Dreyer, K., Ti(C,N) Cermets—metallurgy and properties. *Int. J. Refr. Met. & Hard Mat.*, 1995, **13**, 343–351.
5. Pastor, H., Titanium-carbonitride-based hard alloy for cutting tools. *Mat. Sci. Eng.*, 1988, **A105/106**, 401–411.
6. Richter, V. and Ruthendorf, M. Composition, microstructure, properties and cutting performances of cermets. In: *Proceedings*

of Euro PM '99 Conference on Advances in Hard Materials Production, 1999, pp. 229–236.
7. Errico, G. E., Bugliosi, S. and Guglielmi, E., Tool life reliability of cermet inserts in milling tests. *J. Mater. Proc. Technol*, 1998, **77**, 337–343.
8. Park, D.-S. and Lee, Y.-D., Effect of carbides on the microstructure and properties of Ti(C,N) based ceramics. *J. Am. Ceram. Soc*., 1999, **82**(11), 3150–3154.
9. Ahn, S-Y., Kim, S-W. and Kang, S., Microstructure of Ti(C,N)–WC–NbC–Ni cermets. *J. Am. Ceram. Soc*., 2001, **84**(4), 843–849.
10. Lindahl, P., Gustafson, P., Rolander, U., Stals, L. and Andren, H.-O., Microstructure of model cermets with high Mo or W content. *Int. J. Refr. Met. & Hard Mat*., 1999, **17**, 411–421.
11. Ahn, S., Y, & Kang, S. *Formation of core/rim structure in Ti(C,N)–WC–Ni cermets via a dissolution and precipitation process. J. Am. Ceram. Soc*., 2000, **83**(6), 1489–1494.
12. Laoui, T. and Van der Biest, O., Effect of TiC addition on the microstructure and properties of Ti(C,N)–WC–Co–Ni cermet. *J. Mat. Sci. Lett*., 1994, **13**, 1530–1532.
13. Kang, S., Some issues in Ti(CN)–WC–TaC cermets. *Mat. Sci. Eng*., 1996, **A209**, 306–312.
14. Chen, L., Lengauer, W., Ettmayer, P., Dreyer, K., Daub, H. W. and Kassel, D., Fundamentals of liquid phase sintering for modern cermets and functionally graded cemented carbonitrides (FGCC). *Int. J. Refr. Met. & Hard Mat*., 2000, **18**, 307–322.
15. Jha, A. and Yoon, S. J., Formation of titanium carbonitride phases via the reduction of TiO_2 with carbon in the presence of nitrogen. *J. Mat. Sci*., 1999, **34**, 307–322.
16. Berger, L.-M., Gruner, W., Langholf, E. and Stolle, S., On the mechanism of carborthermal reduction processes of TiO_2 and ZrO_2. *Int. J. Refr. Met. & Hard Mat*., 1999, **17**, 235–243.
17. Xiang, J., Xie, Z., Huang, Y. and Xiao, H., Synthesis of Ti(C,N) ultrafine powders by carbothermal reduction of TiO_2 derived from sol-gel process. *J. Eur. Ceram. Soc*., 2000, **20**, 933–938.
18. Grami, M. E. and Munir, T. Z., The mechanism of combustion synthesis of titanium carbonitride. *J. Mat. Res*., 1994, **9**(2), 431–435.
19. Liuying, M., Huayi, L., Hengzhen, B. and Guochun, L., Influence of CH_4/N_2 ratio on microstructure and mechanical properties of PCVD-Ti(C_xN_{1-x}) coating. *Int. J. Refr. Met & Hard Mat*., 1995, **13**, 369–374.
20. Levi, G., Kaplan, W. D. and Bamberger, M., Structure refinement of titanium carbonitride (TiCN). *Materials Letters*, 1998, **35**, 344–350.
21. Jung, I-J., Kang, S., Jhi, S-H. and Ihm, J., A study of the formation of Ti(CN) solid solutions. *Acta Mater*., 1999, **47**(11), 3241–3245.
22. Azaroff, L. V. and Buerger, M. J., *The Powder Method*. McGraw-Hill, New York, 1958.
23. Roine, A., *HSC Chemistry 4.1, 1999*. Outokumpu Research Oy, Pori, Finland, 1999.
24. Evans, A. G. and Charles, E. A., Fracture toughness determination by indentation. *J. Am. Ceram. Soc*., 1976, **59**, 571–574.
25. Monteverde, F., Medri, V. and Bellosi, A., Synthesis of ultrafine titanium carbonitride powders. *Appl. Organometal. Chem*., 2001, **15**, 421–429.
26. Laoui, T., Zou, H. and Van der Biest, O., Analytical electron microscopy of the core/rim structure in titanium carbonitride cermets. *Refr. Met. & Hard Mat*., 1992, **1992**, 11 207–212.
27. Zhang, S., Qin, C. D. and Lim, L. C., Solid solution of WC and TaC in Ti(C,N) as revealed by lattice parameter increase. *Int. J. Refr. Met. & Hard Mat*., 1993, **12**–1994, 329–333.
28. Jonsson, S., Assessment of the Ti–W–C system and calculations in the Ti–W–C–N. *Zeit. Metallkd*, 1996, **87**(8), 788–795.
29. Gustafson, P. and Östlund, A., Binder-phase enrichment by dissolution of cubic carbides. *Int. J. Refr. Met. & Hard Mat*., 1993, **12**–1994, 129–135.
30. Yang, Q., Lengauer, W., Koch, T., Scheerer, M. and Smid, I., Hardness and elastic properties of Ti(C_XN_{1-X}), Zr(C_XN_{1-X}) and Hf(C_XN_{1-X}). *J. Alloys Compounds*, 2000, **309**, L5–L9.